Anal. Bioanal. Electrochem., Vol. 15, No. 3, 2023, 184-197
https://www.doi.org/10.22034/abec.2023.703900

Analytical & Bioanalytical Electrochemistry

www.abechem.com

Full Paper

Electrochemical Reduction of 2-Substituted Quinoxalines in Aprotic Medium and in Conditions of Protonation

Anton Tsmokalyuk,[1] Polina Mozharovskaia,[1,*] Ekaterina Belina,[1] Ivan Balin,[1] Emiliya Nosova,[1,2] Anatoly Matern,[1] and Alisa Kozitsina[1]

[1]*Institute of Chemical Engineering, Ural Federal University, Mira 28, Yekaterinburg, Russia, 620002*
[2]*I. Ya. Postovsky Institute of Organic Synthesis, Ural Branch of the Russian Academy of Sciences, S. Kovalevskaya Str., 22, Yekaterinburg, Russia, 620108*

*Corresponding Author, Tel.: +7(343)3754895
E-Mail: pnmozharovskaia@urfu.ru

Received: 25 November 2022 / Received in revised form: 3 March 2023 / Accepted: 16 March 2023 / Published online: 31 March 2023

Abstract- The present work is devoted to the electrochemical reduction study of presumably biologically active 2-substituted quinoxaline derivatives. In this work, two new quinoxaline derivatives are presented. The electrochemical behavior of this compound in an aprotic medium and while its protonating was investigated *via* a voltammetric method. Using computational methods, the localization of the reduction centres depending on the compound's structure was determined. The EPR spectra data obtained by electrochemical generation reduction product proved that the studied quinoxaline's electroconversion occurs with radical anion formation. The linear correlation between the reduction potential of studied compounds and energy of their affinity to the electron was found (R^2 = 0.933). This confirms the single reduction mechanism of radical nature for the entire series of studied 2-substituted quinoxaline derivatives. Based on that, the electron-accepting ability of these compounds was compared in order to evaluate their possible bioactivity and to select the most perspective ones among them for further research.

Keywords- Quinoxalines; Cyclic voltammetry; EPR spectroscopy; DFT calculations; Electroreduction

1. INTRODUCTION

The constant variability of virus strains, the growth in the incidence and death from cancer and tuberculosis, the increase in the proportion of primary incidence of mental disorders, as well as the resistance of existing drugs, leads to the need to create new, more effective drugs. Pharmaceuticals whose active ingredients contain a quinoxaline moiety in their scaffold are of great interest because they have a wide range of biological activity, namely anticancer, antidepressant, antipsychotic, antidiabetic, antioxidant, antifungal, antiviral, antimicrobial and antituberculosis [1]. Natural and synthetic quinoxalines are active ingredients of the diverse drugs such as Echinomycin, Levomycin, Actinomycin, Quinacillin, Brimonidine and Varenicline [2,3].

Considering the quinoxaline scaffold essential and widespread use in medical chemistry, synthesis of new quinoxaline derivatives and study of their chemical and biological properties are important strategies for research into new drugs. It is possible to obtain many useful compounds for chronic and metabolic diseases treatment by modifying quinoxaline's structure.

Some previous studies of the quinoxaline derivative's electrochemical behavior have shown that there is a correlation between electrochemical properties and biological activity of these compounds, namely their reduction potential and IC_{90} values against such agents as *Staphylococcus aureus, Proteus Vulgaris* [4] and *Mycobacterium tuberculosis* [5]. It was stated that the quinoxaline derivatives with the least negative reduction potential are the most biologically active [4-6]. Therefore, the study of quinoxalines by electrochemical methods can be useful for evaluating the prospects of synthesized quinoxalines in terms of their biological activity.

Particular attention was paid to the electrochemical conversion mechanism determining. It was noted that the process of reduction of quinoxaline derivatives showing antimicrobial and antitumor activity is characterized by a single-electron transfer and has a radical nature [4-8].

We have found that some derivatives of 2-substituted quinoxalines with photoluminescent properties [9] are structurally similar to quinoxalines, which exhibit antimicrobial activity [4]. However, the redox transformation of these compounds has not been previously studied, and the information obtained may be useful for future studies of the possible biological activity of compounds.

The aim of this work is the expansion of the series of 2-substituted quinoxalines with new derivatives and the study of their electrochemical behavior in an aprotic medium as well as in conditions of protonation. The solution of this aim allows to obtain information about the electron-acceptor ability of the studied compounds.

2. EXPERIMENTAL SECTION

2.1. Test compounds

Eight 2-substituted quinoxaline derivatives were synthesized for the study. The studied compounds can be broken down into three groups basing on their structure arylvinylquinoxalines **I,** quinoxaline-2-carboxalidine-2-aminophenols **II** and (quinoxaline-2-yl)methylenehydrazides **III** (Figure 1).

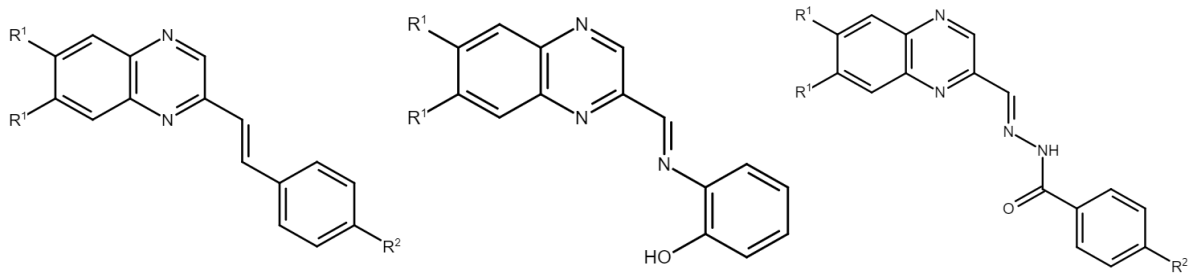

I
a: $R^1 = F$, $R^2 = H$
b: $R^1 = F$, $R^2 = OCH_3$
c: $R^1 = H$, $R^2 = CH_3$
d: $R^1 = H$, $R^2 = NO_2$

II
a: $R^1 = F$
b: $R^1 = H$

III
a: $R^1 = F$, $R^2 = H$
b: $R^1 = H$, $R^2 = t$-Bu

Figure 1. Structural formulas of studied compounds

The synthesis of arylvinylquinoxalines **Ia,b** was carried out by the Knoevenagel condensation of 2-methyl-6,7-difluoroquinoxaline with the corresponding arenecarbaldehyde in glacial acetic acid in the presence of anhydrous sodium acetate [10]. This way did not allow to obtain **Ic,d** derivatives. For this reason, the conditions described for the synthesis of 2-(4-methoxystyryl)quinoxaline were chosen [11].

(*E*)-2-(4-Nitrostyryl)quinoxaline (Id). To a solution of 2-methylquinoxaline (0.609 mL, 6.28 mmol) in acetic anhydride (15 ml) 4-nitrobenzaldehyde (1.404 g, 9.29 mmol) was added. The mixture was refluxed in argon atmosphere for 12 hours, then cooled and red-brown solid was filtered off and washed with ethanol. Yield 1.50 r (86%), mp 186-188 ^oC. ^1H NMR, δ, ppm: 7.78 d (1H, J 16.5 Hz, CH=), 7.78-7.84 m (2H, benzo), 8.01 d (2H, H-2', H-6', J 8.8 Hz), 8.05-8.08 m (2H, benzo), 8.10 d (1H, J 16.5 Hz, CH=), 8.28 d (2H, H-3', H-5', J 8.8 Hz), 9.24 s (1H, H-3). ^{13}C NMR, δ, ppm: 123.97, 128.38, 128.86, 128.96, 129.81, 130.59, 133.59, 141.26, 141.70, 142.49, 145.25, 147.26, 149.85. MS, I_{rel} (%): 277 (91) $[M]^+$, 276 (100), 231 (39), 230 (80), 229 (33), 203 (12), 115 (15), 103 (12), 102 (20), 101 (14), 77 (16), 76 (32), 75 (14), 51 (11), 50 (17). IR (cm^{-1}): 606.36, 690.54, 744.66, 772.51, 834.01, 869.49, 968.01, 1104.33, 1202.33, 1338.88, 1413.42, 1507.63, 1537.96, 1589.21, 1649.62, 1885.44, 2439.29, 3053.44, 3688.26. Found, %: C 69.37, H 4.07, N 15.09. $C_{16}H_{11}N_3O_2$. Calculated, %: C 69.31, H 4.00, N 15.15.

(*E*)-2-(4-Methylstyryl)quinoxaline (Ic) was synthesized by the same method. Yield 77%, mp 119-121 ^oC [lit. 116-118 ^oC [12] ^1H NMR, δ, ppm: 2.40 s (3H, CH_3), 7.25 d (2H, H-3', H-5', J 8.4 Hz), 7.45 d (1H, J 16.4 Hz, CH=), 7.62 d (2H, H-2', H-6', J 8.4 Hz), 7.74-7.80 m (2H, H-

6, H-7), 7.95 d (1H, J 16.4 Hz, CH=), 8.00-8.03 m (2H, H-5, H-8), 9.16 s (1H, H-3). ^{13}C NMR, δ, ppm: 20.95, 124.39, 127.46, 128.73, 128.81, 129.30, 129.52, 130.42, 133.12, 136.09, 138.97, 140.85, 141.72, 145.14, 150.76. MS, I_{rel} (%): 246 (59) $[M]^+$, 245 (100), 231 (31), 115 (18). IR (cm^{-1}): 754.12, 802.99, 959.56, 1122.30, 1309.48, 1409.20, 1539.07, 1600.17, 1931.64, 2355.20, 3034.42. Found, %: C 82.78, H 5.65, N 11.44. $C_{17}H_{14}N_2$. Calculated, %: C 82.90, H 5.73, N 11.37.

Compounds **IIa,b** and **IIIa** were synthesized based on quinoxaline-2-carboxaldehyde when it reacted in ethanol with 2-aminophenol [13] and benzohydrazide [14], respectively. 4-*t*-Butylhydrazide was involved in the reaction with quinoxaline-2-carboxaldehyde to give a new **IIIb** derivative.

4-*t*-Butylbenzoic acid (quinoxalin-2-yl)methylenehydrazide (**IIIb**). The solution of 4-*t*-butylhydrazide (0.304 g, 1.58 mmol) in ethanol (15 mL) was added in portions to the solution of quinoxalin-2-carbaldehyde (0.25 g, 1.58 mmol) in ethanol (25 mL). The reaction mixture was refluxed for 10 h and then concentrated in vacuo. The precipitate was filtered off and recrystallized from ethanol. Yield 0.41 г (78%), mp 216-218 ºC. ^{1}H NMR, δ, ppm: 1.38 s (9H, CMe_3), 7.54 d (2H, H-3', H-5'. J 7.5 Hz), 7.84-7.86 m (2H, Ar), 7.90 d (2H, H-2', H-6'. J 7.5 Hz), 8.09-8.11 m (2H, Ar), 8.66 s (1H, H(3)), 9.54 s (1H, CH=N), 12.2 s (1H, NH). ^{13}C NMR, δ, ppm: 30.85, 34.73, 125.35, 127.70, 128.98, 129.06, 130.8, 130.62, 130.76, 141.26, 141.56, 142.79, 145.57, 148.50, 155.13, 163.46. MS, I_{rel} (%): 332 (4) $[M]^+$, 171 (54), 162 (17), 161 (100), 146 (16), 143 (21), 118 (25), 102 (14), 91 (15). IR (cm^{-1}): 550.59, 583.33, 600.94, 702.87, 732.78, 761.98, 782.64, 848.04, 880.14, 919.27, 943.06, 1014.65, 1071.58, 1123.51, 1152.12, 1192.31, 1268.20, 1298.28, 1349.05, 1403.37, 1488.44, 1537.92, 1557.64, 1608.00, 1654.75, 2878.81, 2963.85, 3227.55. Found, %: C 72.35, H 6.11, N 16.79. $C_{20}H_{20}N_4O$. Calculated, %: C 72.27, H 6.06, N 16.86.

Unless otherwise indicated, all common reagents and solvents were used from commercial suppliers without further purification. Melting points were measured on the instrument Boetius. The method of thin-layer chromatography was used to monitor the progress of the reaction. The column chromatography was carried out on SiO_2. ^{1}H NMR and ^{13}C NMR spectra were recorded at room temperature at 300 and 75.3 MHz respectively, on a Bruker AC-300 spectrometer; at 400 and 100 MHz respectively, on a Bruker DRX-400 spectrometer. Mass spectra were recorded on the SHIMADZU GCMS-QP2010 Ultra instrument with electron ionization (EI) of the sample. The elemental analysis was carried out on an automated Perkin Elmer PE 2400 series II CHNS analyzer. IR spectra were measured using a Perkin Elmer Spectrum 65instrument equipped with a Quest ATR Accessory (Specac) by attenuated total reflectance (ATR) in the range of 400–4000 cm^{-1}.

2.2. Chemicals

An aprotic chemically pure dimethylsulfoxide (hereinafter DMSO) produced by ECOS-1 (Russia) with a water content of no more than 0.1% was used as a solvent. For medium protonation, a concentrated (35-38%) hydrochloric acid (Sigma Tech, Russia) was used. 99% tetrabutylammonium tetrafluoroborate (hereinafter Bu_4NBF_4) and ferrocene produced by Sigma-Aldrich (Switzerland) were used for various applications. Oxygen from solutions was removed by blowing with an inert gas argon 99.9% purity.

2.3. Electrochemistry

The electrochemical studies were carried out in a standard three electrode cell using potentiostat/galvanostat Autolab Type III (Metrohm, Switzerland) complete with a magnetic strirrer. The indicator electrode was glassy carbon electrode disk with diameter of 3 mm (S= 7.065 mm^2). The surface of the working electrode was mechanically cleaned on a fabric substrate soaked with aluminum oxide with before each measurement. An $Ag/AgCl_2/KCl_{sat}$/DMSO membranes was used as a reference electrode, and a graphite electrode was used as the auxiliary electrode.

To study the effect of protonation on the studied compounds' Red-Ox properties a mixture of HCl and DMSO in a ratio of 1:19 was sequentially added to the analyzed solution by 10 μL portions.

2.4. EPR spectroscopy

The study of the electrochemically generated reduction product of the compound **Ia** was carried out by the EPR spectroscopy using the ELEXSYS E500 EPR spectrometer.

After electrolysis of the compound **Ia** radical at different concentrations (0.1-0.3 M) and accumulation time (300-1800 s). The resulting solution was taken into a glass capillary. This capillary was placed in a quartz cell, which was then installed in the resonator of the spectrometer with registration parameters: magnetic field - 351.3 mT with a sweep range of 80 mT and a modulation amplitude of 0.6 mT.

2.5. Quantum chemical calculations

Quantum-chemical calculations of the optimized structures, energy, electron density and the EPR spectra of the molecules were performed by the b3lyp hybrid method [15,16] in the def2-TZVP basis [17], taking into account Coulomb splitting [18], Atom-pairwise Dispersion Correction [19,20] and using conductor-like polarizable continuum model (C-PCM) for solvent effects [21] in the ORCA 4.2.1 program [22–24]. TightSCF convergence has been applied. To search for stationary points on the potential energy surfaces, a complete geometry optimization was carried out using the TightOpt convergence criteria and checking natural frequencies.

Preview of Fukui's functions [25] and execution electrostatic potential maps in GaussView6.0 [26].

3. RESULTS AND DISCUSSION

3.1. Electrochemical behavior

The electrochemical behavior of compounds **Ia-c**, which are structural analogs and differ only in substituents, was studied by the cyclic voltammetry (CV) method in a DMSO background solution with the addition of 0.1 M Bu_4NBF_4.It follows from the CV data that compounds **Ia-c** have a similar CV shape. In this case, the form of CV **Ic** is identical for **Ia** and **Ib**; and curves **IIa,b** and **IIIa,b** are pairwise identical. The exception is **Id**, the voltammogram of which is given separately. Therefore, **Fig. 2** shows the CV of one compound from each group, and 1 reversible recovery peak, which is located in the range -2 < E < -1 V, is observed. Data on the characteristics of the peaks are presented in **Table 1.** To determine the effective number of electrons n_e, involved in the first stage of electrochemical reduction, the current of the compound in DMSO on CV was compared with the current calculated by the Rendles–Shevchik equation for reversible electrochemical reactions and the current and area of the standard reversible ferrocene redox system under the same conditions [27]. The obtained value of n_e for all compounds, determined by all used electroanalytical methods, was 1e, which corresponds to the reduction of the quinoxaline fragment of the studied compounds, since unsubstituted quinoxaline and some of its derivatives are reduced in a similar way [28,29].

Table 1. Reduction peaks of compounds **I-III** description*

Compound	E_p^{iC}. V		I_p^A/I_p^C	ΔE_p. V	$I_p^{iC}\cdot10^5$. A	$Q\cdot10^6$. C
Ia	k = 1	-1.30	0.99	0.058	1.33	4.22
Ib	k = 1	-1.33	0.99	0.059	1.43	5.26
Ic	k = 1	-1.45	0.99	0.057	1.49	4.38
Id	k = 1	-0.85	0.98	0.066	1.21	10.94
	k = 2	-1.20	0.96	0.064	1.38	
	k = 3	-2.39	Irreversible peak		6.07	17.74
IIa	k = 1	-0.99	0.91	0.24	1.15	8.48
	k = 2	-1.58	0.98	0.060	1.36	
IIb	k = 1	-1.00	0.89	0.27	1.16	8.72
	k = 2	-1.68	0.97	0.062	1.46	
IIIa	k = 1	-1.19	0.87	0.25	1.40	8.66
	k = 2	-1.46	0.96	0.058	1.45	
IIIb	k = 1	-1.20	0.85	0.29	1.23	8.26
	k = 2	-1.56	0.95	0.058	1.22	

*For unsubstituted quinoxaline E_p^C = -1.61 V. $I_p^C = 1.40\cdot10^{-5}$ A. Q = $5.31\cdot10^{-6}$ C (similar registration parameters as for test compounds)

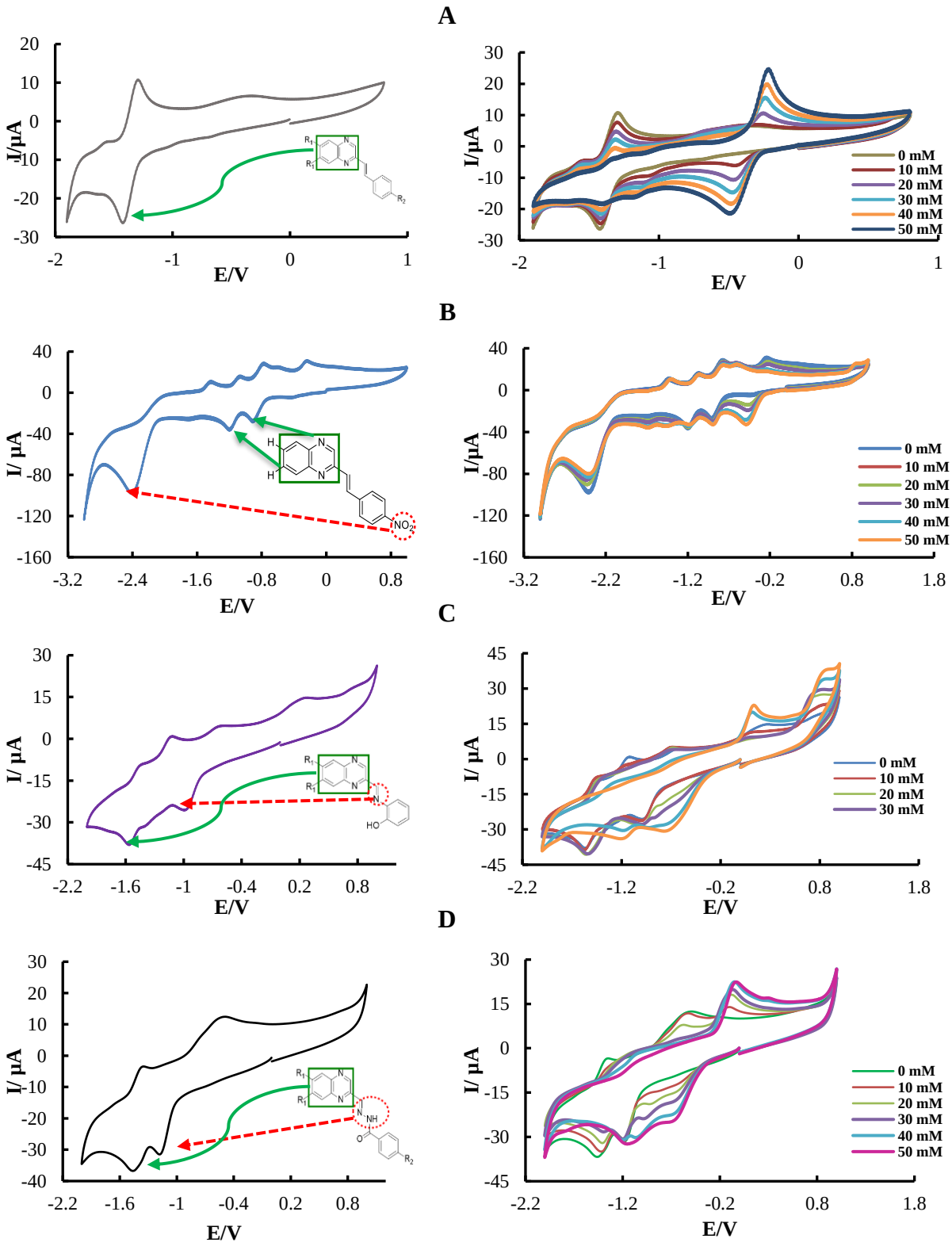

Figure 2. CVs obtained in the presence of 2 mM compound **Ic** (A). **Id** (B). **IIa** (C) and **IIIa** (D) in a DMSO solution with 0.1 M Bu_4NClO_4 (on the left) and during medium protonation by 10 μL portions of HCl/DMSO mixture (on the right) using glassy carbon electrode (S=7.065 mm^2). Scan rate 100mVs^{-1}. Potentials were measured relative to $Ag/AgCl/KCl_{sat}$/DMSO.

To establish the kinetic parameters of the process, the electrochemical behavior of **Ia**, **IIa, IIIa** was studied using the chronoamperometry (CA) and CV methods. Logarithmic analysis of the chronoamperograms of compound **Ia** at E = -1.4V, **IIa** at E = -1.05V and **IIIa** at E = -1.25V showed that the slope of the lg(I)-lg(τ) graph in the interval 1<t<2c is in the range from -0.49 to -0.50, which is close to the value characteristic of a diffusion-controlled electrochemical reaction (-0.5) [27]. Moreover, the electroreduction peak current on the CV curves grows linearly from the root of the potential scan rate, which also confirms the diffusion kinetics [30]. This is confirmed by the coefficient of determination, which for all three selected compounds is 0.9999.

As for **Ia-c** protonation, it causes a gradual decrease of the initial reduction peak and related equivalent growth of another cathodic peak with the potential shift to -1 < E < 0 V.

In addition to characteristic for **Ia-c** reduction stage, the electrochemical conversion of **IIa,b** as well as **IIIa,b** (Figure 2B-C) contains another one cathodic peak located in the range of (-0.9; -1.2) V (**Table 1**). According to the previous data [31,32], this first peak of reduction is presumably related with the C=N bond reduction. Using the same approach of the kinetics type and transferred electrons number determination, it was found that the reduction of these compounds is also a 1-electron process limited by diffusion [33]. The research also showed that **IIa,b** first reduction potential is higher than one of **IIIa,b**. It is probably connected to the greater electron-accepting capacity of C=N compared to C=N–N through the redistribution of the electron density in the exocyclic chain.

While acidifying the medium of **IIa,b** and **IIIa,b**, the second reduction peak changes in the manner described for **Ia-c** and, oppositely , the first one's potential remains without changes. Moreover, the mechanism of reduction **IIa,b** did not changed by adding the first portions H^+. That effect was presumably caused by the hydroxyl group, which is protonated first since its oxygen atom is more electronegative than quinoxaline's nitrogen.

Based on the obtained information, it was assumed the localization of the reduction centres depending on the compound's structure. The **Ia,b** reversible Red-Ox process occurs with the participation of the pyrazine C=N bonds; additionally imino group in **IIa,b** and hydrazono group in **IIIa,b** irreversibly reduce. Protonation facilitates the reduction of the quinoxaline fragment due to its larger electronegativity in comparison with the exocyclic C=N bonds, which is confirmed by calculations. Furthermore, the pyrazine C=N bonds are less electron-deficient than the exocyclic ones and reduce secondarily. which is due to the presence of a π-conjugated system of quinoxaline and its partial electron saturation. Therefore, it was suggested that the first reduction peak corresponds to the process occurring at the exocyclic C=N bonds, the second one – at the quinoxaline fragment. Schematically. this can be presented as shown in the Figure 2 on the left side.

The electrochemical conversion of **Id** slightly differs from that of other compounds (Figure 2B), which is caused by the presence of a strong electron-accepting substituent. There is an

assumption that nitro group pulls the electron density displacing it from the quinoxaline scaffolds. Then, due to the electron density lack, both pyrazine C=N bonds reduce, and it is reflected by two reversible 1-electron reduction peaks at potentials of -0.85 and -1.20 V (Table 1). Comparatively high values of these potentials mean that the electron-accepting group contributes to the quinoxaline reduction process to proceed more easily. Consequently, being saturated with electron density, irreversible 4-electron reduction of nitro group [34,35] occurs after the quinoxaline fragment's one. Since nitro group is considerably electronegative, its cathodic peak decrease with the potential shift to ~ -0.5 V with protonation, making quinoxaline's reduction peaks less resolution.

3.2. Radical nature of reduction

The selection of electrochemical parameters for the EPR spectrum registration was made. The optimal conditions for paramagnetic products electrolysis: 0.3 mM of the test compounds. Time for accumulation is 900 s at the potential of ~ -2.0 V. An increase of the generation time to 1800 s does not lead to a growth of the signal intensity. Therefore, it might be concluded that the radical's lifetime is less than 1800 s. Also, an experiment without electrogeneration was conducted, unfortunately, it did not provide any satisfactory results.

As a result, the EPR spectrum of the electrochemically generated reduction product of **Ia** was detected (Figure 3). Noteworthy, that the EPR spectrum calculated by the DFT method for corresponding radical anion, based on its spin density distribution, is close to those obtained experimentally.

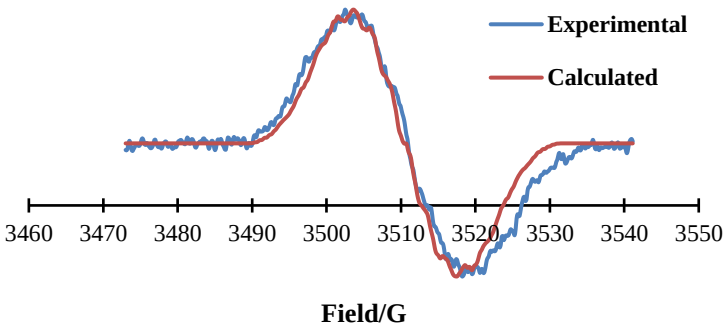

Figure 3. EPR spectrum of compound **Ia** radical anion

3.3. Single electrochemical reduction mechanism

Based on the Fukui function calculated by the DFT method for selected molecules during the reduction process, it becomes possible to determine the highest probability of localization of the transferred electron in the structure of the molecule [36]. Considering the similarity of the Fukui function for structural analogues (with the exception of Id), Figure 4 shows the Fukui function for compounds from each group. It is also possible to conclude from Figure 4 that the

electrochemical reduction of the C=N bond of the pyrazine ring and the imino, hydrazone or nitro groups are considered the most likely processes for the selected compounds.

Nitro group of **Id** has strong electron-accepting properties and also is a reduction center together with the quinoxaline fragment. Therefore, the distribution of the electron density of the transferred electron occurs in both reduction centers. However, if the reduction of the pyrazine C=N bond requires a 1-electron Red-Ox transfer, then the reduction of the nitro group requires a larger number of electrons, which implies more energy costs. Therefore, it can be assumed that the pyrazine bonds in the quinoxaline fragment are reduced first, while the reduction of the nitro group continues at more negative potential values.

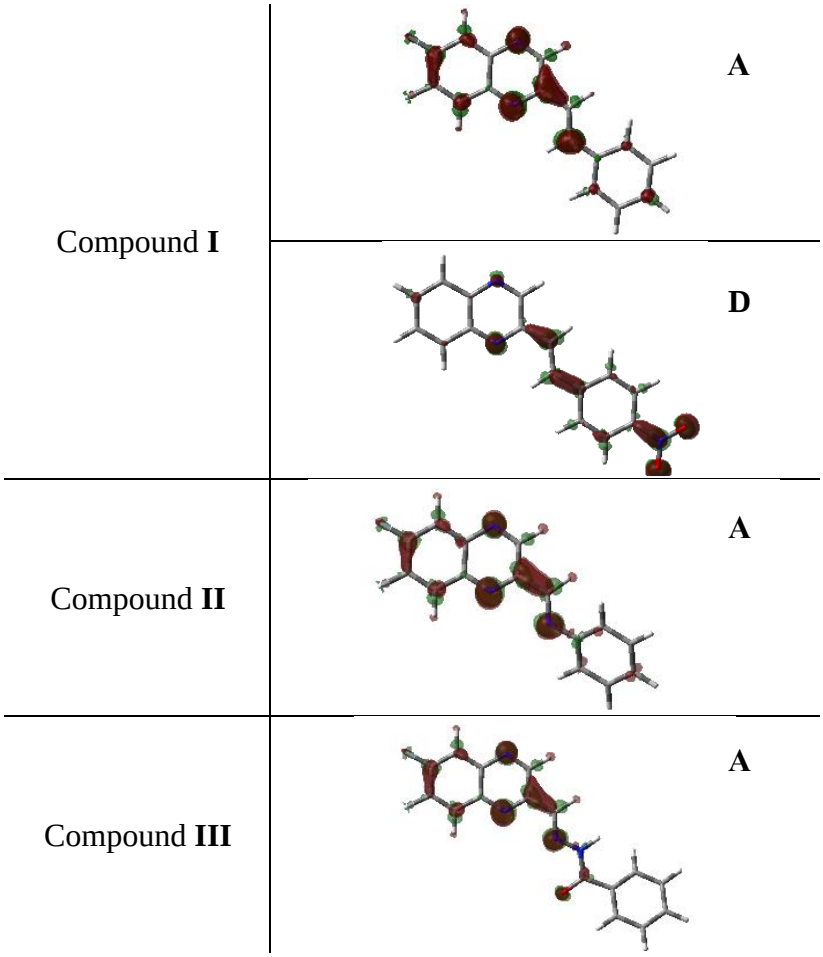

Figure 4. Fukui function $f+$ for studied compounds

Considering the similarity of the electron density in the Higher Occupied Molecular Orbital of the radical anions and the distribution of the Fukui function for the corresponding molecules, as well as the coincidence of the experimental and calculated EPR spectra of the radical anions of compound **Ia**, an assumption was made about a similar mechanism for the electrochemical reduction of compounds. To describe the electron-accepting ability of the studied compounds their adiabatic energy of affinity to the electron (EA_{ad}) was calculated by the energy difference

between a neutral molecule and its radical anion. The linear correlation of EA_{ad} on the test compounds and unsubstituted quinoxaline first reduction potentials was found. The obtained data are shown in the Figure 5.

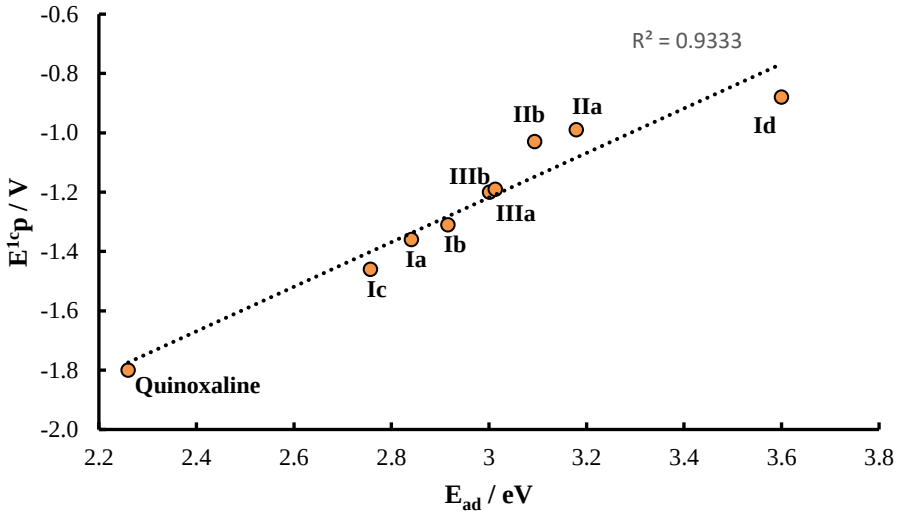

Figure 5. Correlation between EA_{ad} and first reduction potentials of unsubstituted quinoxaline and its studied derivatives

The fact that the resulting regression of the dependence has a high correlation factor confirms the single mechanism of electrochemical reduction process for the whole series of test compounds. Moreover, it justifies the radical nature of all studied compounds' reduction (except **Id)** along with **Ia** and unsubstituted quinoxaline because the latter reduce with radical anions formation (for unsubstituted quinoxaline proven by [28]).

4. CONCLUSION

Based on the established similarity of the structure of 2-substituted quinoxalines, previously studied in terms of photophysical properties [9], and quinoxalines that exhibit antimicrobial action, it is assumed that these compounds may be biologically active. Consequently, this series of 2-substituted derivatives was expanded with new synthesized compounds and taken for the study of electrochemical behavior.

In the studied series of quinoxaline derivatives, the localization of electroreduction centers was correlated with their structure. Depending on the different functional groups used, the Red-Ox process occurs with the participation of the C=N bonds of pyrazine ring, imino, hydrazono or nitro groups.

It was found that the unsubstituted quinoxaline and compound **Ia** electrochemical reduction corresponds to the formation of the radical anions. Also, the linear correlation of EA_{ad} on the test compounds and unsubstituted quinoxaline first reduction potentials was found. Based on

this it is possible to suggest the single reduction mechanism of radical nature for all studied compounds. Overall, the scheme on Figure 6 of the studied compounds electrochemical reduction might be illustrated as:

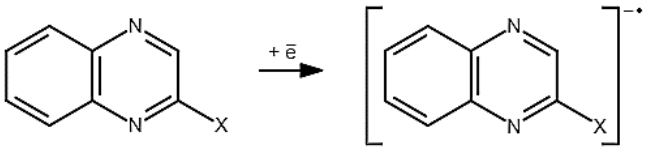

Figure 6. The probable scheme of electroreduction of the studied compound

The effect of protonation on the electrochemical reduction of test compounds has been studied. It might be essential for understanding the processes occurring in aqueous media and biological fluids. The experiments showed that the medium acidifying facilitates the reduction of the compounds.

To conclude, the test compounds might be arranged in a row of their electrochemical activity: **Ic – Ib – Ia – IIIb – IIIa – IIb – IIa – Id** with **Id** having the highest reduction ability. Considering the electroconversion similitude of the compounds presented in this work and the ones exhibiting antimicrobial effects [4,6]. It is possible to assume that the studied compounds are bioactive. Therefore, the sequence of the 2-substituted quinoxaline derivatives potential bioactivity increases in accordance to their chemical activity and coincides with the row presented. As a result, compounds **IIa** and **Id** might show comparatively the greatest bioactivity what makes them prospective for the future studies.

Acknowledgements

This work was financially supported by the Russian Foundation for Basic Research (Project No. 19-29-08015mk).

Declarations of interest

The authors declare no conflict of interest in this reported work.

REFERENCES

[1] A. Nandikolla, Y.M. Khetmalis, K.M. Naidu, B.K. Kumar, S. Murugesan, and K.V.G.C. Sekhar, Toxicol. In Vitro. 82 (2022) 105370.

[2] J.A. Pereira, A.M. Pessoa, M.N.D.S Cordeiro, R. Fernandes, and C. Prudencio, J. P. Noronha, M. Vieira, Eur. J. Med. Chem. 97 (2015) 664.

[3] M.S.F. Franco, M.H. de Paula, P.C. Glowacka, F. Fumagalli, G.C. Clososki, and F. da Silva Emery, Tetrahedron Lett. 59 (2018) 2562

[4] P.W. Crawford, R.G. Scamehorn, U. Hollstein, M.D. Ryan, and P. Kovacic, Chem.-Biol. Interact. 60 (1986) 67.
[5] E. Moreno, S. Pérez-Silanes, S. Gouravaram, A. Macharam, S. Ancizu, E. Torres, I. Aldana, A. Monge, and P.W. Crawford, Electrochim. Acta 56 (2011) 3270.
[6] M. D. Ryan, R. G. Scamehorn, and P. Kovacic, J. Pharm. Sci. 74(4) (1985) 492.
[7] S. Perez-Silanes, G. Devarapally, E. Torres, E. Moreno-Viguri, I. Aldana, A. Monge, and P.W. Crawford, Helv. Chim. Acta 96 (2013) 217.
[8] E.M. Miller, Q. Xia, M.E. Cella, A.W. Nenninger, M.N. Mruzik, K.A. Brillos-Monia, Y.Z. Hu, R. Sheng, C.M. Ragain, and P.W. Crawford, Molecules. 22 (2017) 1442.
[9] E.V. Nosova, S. Achelle, G.N. Lipunova, V.N. Charushin, and O.N. Chupakhin, Russ. Chem. Rev. 88 (2019) 1128.
[10] E.V. Nosova, T.V. Trashakhova, V.S. Ustyugov, N.N. Mochul'Skaya, M.S.Valova, G.N. Lipunova, and V.N. Charushin, Russ. Chem. Bull. 60 (2011) 942.
[11] B.Bachowska, G. Matusiak, Chem. Heterocycl. Compd. (N.Y., NY, U. S.) 45 (2009) 80.
[12] E.N. Gulakova, A.G. Sitin, L.G..Kuz'mina, and O.A. Fedorova, Russ. J. Org. Chem. 47 (2011) 2 245.
[13] E. Nosova, T. Stupina, A. Chupakhin, G. Lipunova, M. Valova, P. Slepukhin, and V. Charushin, Open Chemistry 13 (2015) 1 61.
[14] E.V. Nosova, A.A. Chupakhin, G.N. Lipunova, P.A. Slepukhin, M.S. Valova, and V.N Charushin, Russ. Chem. Bull. 63 (2014) 6 1344.
[15] A. Becke, J. Chem. Phys. 98 (1993) 5648.
[16] C Lee, and W. Yang, Phys. Rev. B: Condens. Matter Mater. Phys. 37 (1988) 785.
[17] F. Weigend, and R. Ahlrichs, Phys. Chem. Chem. Phys. 7 (2005) 3297.
[18] F. Weigend, Phys. Chem. Chem. Phys. 8 (2006) 1057.
[19] S. Grimme, S. Ehrlich, and L. Goerigk, J. Comput. Chem. 32 (2011) 1456.
[20] S. Grimme, J. Antony, S. Ehrlich, and H. Krieg, J. Chem. Phys. 132 (2010) 154104.
[21] D. M. York, and M. Karplus, J. Phys. Chem. A 103 (1999) 11060.
[22] F. Neese, The ORCA program system, Wiley Interdisciplinary Reviews: Computational Molecular Sci. 2 (2012) 73.
[23] F. Neese, Software update: the ORCA program system. version 4.0. Wiley Interdisciplinary Reviews: Computational Molecular Sci. 8 (2018) 1327.
[24] F. Neese, et al. The ORCA quantum chemistry program package J. Chem. Phys.152 (2020) 224108.
[25] R.G. Parr, and Y. Weitao, J. Am. Chem. Soc. 106 (1984) 4049.
[26] T.A. Keith, and J.M. Millam GaussView, Version 6.1, Roy Dennington, Semichem Inc. (2016).

[27] F. Scholz, A.M. Bond, R.G. Compton, et al. Electroanalytical Methods. Guide to experiments and application, Springer: Berlin, Germany (2002) ISBN: 978-3-642-02915-8.
[28] L.A. Shundrin, I.G. Irtegova, N.V. Vasilieva, P.A. Avrorov, N.Y. Selikhova, A.G. Makarov, A.Y. Makarov, Y.G. Slizhov, and A.V. Zibarev, J. Phys. Org. Chem. 30 (2017) 3667.
[29] R.S. Assary, F.R. Brushett, and L.A. Curtiss, RSC Adv. 4 (2014) 57442.
[30] M. Borsari, M. Cannio, and G. Gavioli, Electroanalysis 15 (2003) 1192.
[31] A.J. Fry, and R.G. Reed, J. Am. Chem. Soc. 91 (1969) 6448.
[32] A. Izadyar, K.M. Omer, Y. Liu, S. Chen, X. Xu, and A.J. Bard, J. Phys. Chem. 112 (2008) 20027.
[33] S.U. Pedersen, T.B. Christensen, T. Thomasen, and K. Daasbjerg, J. Electroanal. Chem. 454 (1998) 123.
[34] M. Heyrovsky, and S. Vavricka, J. Electroanal. Chem. 28 (1970) 409.
[35] T. Wirtanen, E. Rodrigo, and S.R. Waldvogel, Adv. Synth. Catal. 362 (2020) 2088.
[36] M. E. Beck, J. Chem. Inf. Model 45 (2005) 2 273.